Progress In Electromagnetics Research B, Vol. 48, 115–130, 2013

SPECTRAL AND TEXTURAL WEIGHTING USING TAKAGI-SUGENO FUZZY SYSTEM FOR THROUGH WALL IMAGE ENHANCEMENT

Muhammad M. Riaz and Abdul Ghafoor*

Department of Electrical Engineering, College of Signals, National University of Sciences and Technology (NUST), Islamabad, Pakistan

Abstract—A through wall image enhancement scheme based on Takagi-Sugeno fuzzy system and principal component analysis is proposed. The scheme incorporates spectral properties of image and textural properties of eigen components of image to assign weights. The scheme overcomes the empirical setting of inference engine and output membership functions. Simulation demonstrates the effectiveness of proposed scheme in terms of accuracy.

1. INTRODUCTION

Image enhancement is an active research area in Through Wall Imaging (TWI) [1–4]. The clutters due to walls and false targets degrade the image quality significantly. Beside the hardware improvements [5–7], many image enhancement schemes (including background subtraction [8], spatial filtering [9], wall parameter estimation/modeling [10, 11], doppler domain filtering [12] and image fusion [13]) are in literature. These schemes have their own drawbacks and limitations (some of them are discussed in [14]).

Recently, statistical schemes like Singular Value Decomposition (SVD), QR Decomposition and Principal Component Analysis (PCA) were proposed for TWI image enhancement [14–21]. These schemes decompose the input image into different subspaces (clutter, target and noise) based on statistical properties [14–21]. Unfortunately extraction of target subspaces requires empirical settings.

Verma et al. [15] proposed that the first subspace represents wall clutter, second subspace represents target(s) and all other subspaces

Received 17 December 2012, Accepted 23 January 2013, Scheduled 24 January 2013
* Corresponding author: Abdul Ghafoor (abdulghafoor-mcs@nust.edu.pk).

belong to noise. However this statement is not always true because the target subspaces are dependent on target characteristics (shape, size and location etc.) [16].

Information theoretic criterion and SVD based scheme [16] was proposed to overcome this limitation. Target subspaces were determined by minimizing the information theoretic criterions (such as Akaike information criterion and minimum description length criterion) on singular values. The scheme was able to detect multiple targets. However due to overlapping boundaries of target and noise singular values, there arises problem of miss and false detection.

Wavelet transform and PCA based scheme [18] was proposed to overcome the problem of miss detection. The scheme first combines the target and noise subspaces and then apply threshold (calculated using eigen values) on different decomposition levels for denoising. The scheme was somehow able to overcome the miss detection problem but at the cost of increased false detection.

Fuzzy logic and statistical methods based TWI image enhancement schemes were proposed to overcome the miss and false detection problem [14, 20, 21]. These schemes [14, 20, 21] enhance targets by combining different subspaces with some weights. Fuzzy logic with Mamdani inference engine is used to assign weights for overlapping boundaries of noise and targets. The input and output Membership Functions (MFs) were adjusted empirically at equal distance and variance [20]. Automatic adjustment of input MFs based on K-means clustering to overcome the empirical adjustment was also proposed [14, 21]. However the parameters for fuzzy inference engine and output MFs were chosen intuitively.

A TWI image enhancement scheme using Takagi Sugeno (TS) fuzzy system and PCA (TSPCA) is proposed. TSPCA scheme incorporates both spectral properties of image and textural properties of eigen components of image to assign weights. The scheme overcomes the empirical setting of inference engine and output MFs. Simulation demonstrates that the proposed scheme minimizes false and miss detection rates.

2. PRELIMINARIES

Here we briefly describe the TWI image enhancement scheme presented in [14]. Let covariance matrix C_G of B-scan image G (having dimensions $K \times L$, $K \leq L$) is given as,

$$C_G = \frac{1}{K} G G^T = \Gamma \Lambda \Gamma^T$$

where, $\Gamma = [\gamma_1, \gamma_2, \ldots, \gamma_K]$ and $\Lambda = \text{diag}[\lambda_1, \lambda_2, \ldots, \lambda_K]$ are eigen vectors and eigen values respectively. The principal component matrix Φ is,

$$\Phi = G^T\Gamma = [\phi_1, \phi_2, \ldots, \phi_K]$$

Image enhancement is performed by decomposing G into clutter G_{cl}, target G_{tar} and noise G_{no} as,

$$G = \underbrace{\sum_{k=1}^{m_1} \gamma_k \phi_k^T}_{G_{cl}} + \underbrace{\sum_{k=m_1+1}^{m_2} \gamma_k \phi_k^T}_{G_{tar}} + \underbrace{\sum_{k=m_2+1}^{K} \gamma_k \phi_k^T}_{G_{no}}$$

It was proposed that $m_1 = 1$ for wall clutter and $m_2 = 2$ for target and rest represent noise [15], i.e.,

$$G_{tar_1} = \gamma_2 \phi_2^T \tag{1}$$

In [14], it was proposed that the target image G_{tar_2} is weighted sum of all eigen components except first component i.e.,

$$G_{tar_2} = \sum_{k=2}^{K} \gamma_k \phi_k^T w_k \tag{2}$$

where w_k are weights assigned on the basis of experimental observation (that high weights for larger eigen values and their larger differences, and vice versa). In [20], Mamdani fuzzy system with product inference engine and center average defuzzifier was used. K-means clustering was used to assign the means and variances of input Gaussian MFs while output Gaussian MFs were placed at equal distance with equal spread [20].

3. PROPOSED TSPCA IMAGE ENHANCEMENT SCHEME

Mamdani fuzzy system (proposed in [20]) involves fuzzification, inference engine and defuzzification steps [22]. The accuracy of weight assignment based on Mamdani fuzzy system mainly depends on the right selection of fuzzifier (Gaussian, singleton and triangular, etc.), inference engine (product, Zadeh, Dienes Rescher and Lukasiewicz, etc.) and defuzzifier (center average, center gravity and maximum, etc.). Furthermore, the accuracy of weight assignment also depends on the statistics (means and variances) of output MFs. In contrast to input MFs the statistics of output MFs can not be determined from input histogram.

Mamdani fuzzy systems are also not time efficient (since they involve fuzzification, inference engine and defuzzification steps). Note also that in [20], weights were assigned only spectral information (eigen values and difference of eigen values). It is observed that the eigen vectors and their corresponding eigen images also contain target related useful information.

Foregoing in view, we propose a scheme (TSPCA) based on TS fuzzy system and eigen image information. The texture features (correlation, energy and homogeneity) are extracted from eigen images and weights are assigned based on spectral and texture features. The target image G_{tar_3} of proposed scheme is,

$$G_{tar_3} = \sum_{k=2}^{K} \frac{1}{2}(\alpha_k + \beta_k)\gamma_k \phi_k^T \tag{3}$$

where α_k, β_k are spectral and textural weights respectively computed for kth eigen image.

3.1. Computation of Spectral Weights

In contrast to spectral weights computed in [20], here we use TS fuzzy system [24]. Let A_α^1, A_α^2 and A_α^3 (represent "High", "Medium"

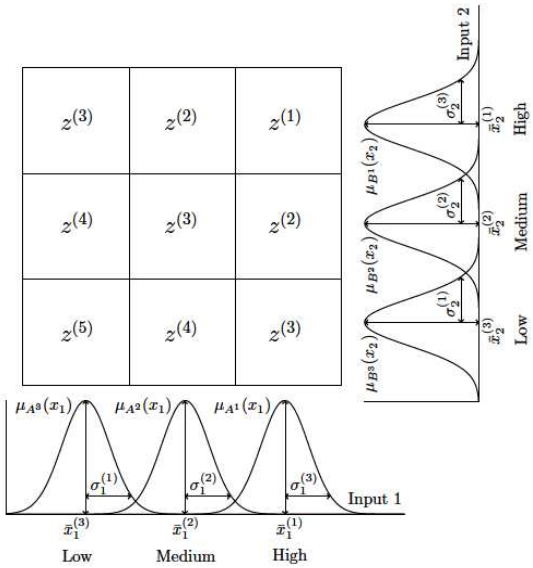

Figure 1. Fuzzy rule base.

and "Low" respectively) are defined for λ_k as shown in Figure 1. The Gaussian MFs are $\mu_{A^1_\alpha}(x_1) = \exp(-(\frac{x_1-\bar{x}_1^{(1)}}{\sigma_1^{(1)}})^2)$, $\mu_{A^2_\alpha}(x_1) = \exp(-(\frac{x_1-\bar{x}_1^{(2)}}{\sigma_1^{(2)}})^2)$ and $\mu_{A^3_\alpha}(x_1) = \exp(-(\frac{x_1-\bar{x}_1^{(3)}}{\sigma_1^{(3)}})^2)$. Similarly, let B^1_α, B^2_α and B^3_α (represent "High", "Medium" and "Low" respectively) are defined for $\Delta\lambda_k = \lambda_k - \lambda_{k+1}$ as shown in Figure 1. The Gaussian MFs are $\mu_{B^1_\alpha}(x_2) = \exp(-(\frac{x_2-\bar{x}_2^{(1)}}{\sigma_2^{(1)}})^2)$, $\mu_{B^2_\alpha}(x_2) = \exp(-(\frac{x_2-\bar{x}_2^{(2)}}{\sigma_2^{(2)}})^2)$ and $\mu_{B^3_\alpha}(x_2) = \exp(-(\frac{x_2-\bar{x}_2^{(3)}}{\sigma_2^{(3)}})^2)$, where $\{x_1, x_2\} \in [0, 1]$. The means $\bar{x}_1^{(i_1)}$, $\bar{x}_2^{(i_2)}$ and variances $\sigma_1^{(i_1)}$, $\sigma_2^{(i_2)}$ (for $\{i_1, i_2\} \in \{1, 2, 3\}$) of fuzzy sets are calculated using K-means algorithm. Eigen values λ_k are clustered into three classes based on histogram (similar procedure is adopted for

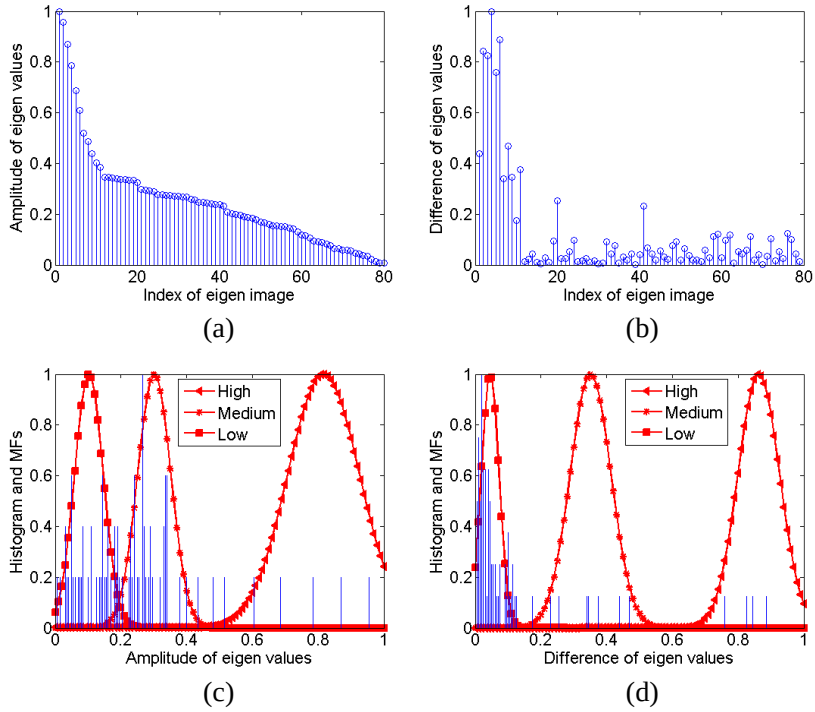

Figure 2. (a) Amplitude of eigen values of B-scan image. (b) Difference of eigen values. (c) MFs and histogram of eigen values. (d) MFs and histogram of difference of eigen values.

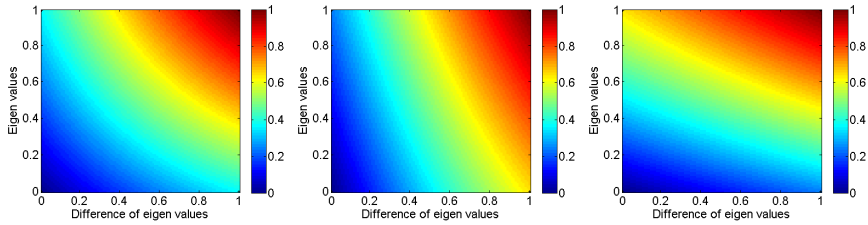

Figure 3. Output spectral weighting function Eq. (4): (a) $\eta_1 = \eta_2 = 0.5$, (b) $\eta_1 = 0.25$ and $\eta_2 = 0.75$, (c) $\eta_1 = 0.75$ and $\eta_2 = 0.25$.

$\Delta\lambda_k$) [23]. The means and variances of each cluster are used as centers $\bar{x}_1^{(i_1)}$, $\bar{x}_2^{(i_2)}$ and spreads $\sigma_1^{(i_1)}$, $\sigma_2^{(i_2)}$ of MFs respectively as shown in Figure 2. The TS rule base for computing spectral weights is,

$$\begin{aligned} &\text{IF } \lambda_k \text{ is } A_\alpha^{(i_1)} \text{ AND } \Delta\lambda_k \text{ is } B_\alpha^{(i_2)} \\ &\text{THEN } z_\alpha^{(i_1+i_2-1)} = \left(\frac{1}{1+e^{-\eta_1\lambda_k}+e^{-\eta_2\Delta\lambda_k}}\right)^{i_1+i_2-1} \end{aligned} \tag{4}$$

where η_1 and η_2 are constants used to control the contribution of λ_k and $\Delta\lambda_k$. This rule base is shown in Figure 3 for $i_1 = i_2 = 1$ (Figure 3(a) for $\eta_1 = \eta_2 = 0.5$, Figure 3(b) for $\eta_1 = 0.25$ and $\eta_2 = 0.75$ and Figure 3(c) for $\eta_1 = 0.75$ and $\eta_2 = 0.25$). Note that when $\eta_1 < \eta_2$, the effect of $\Delta\lambda_k$ is dominant compared to λ_k on weights (and vice versa). Further note that large $i_1 + i_2$ reduces the output of rule-base (weight) which is desirable.

The aggregated spectral weight α_k is,

$$\alpha_k = \frac{\sum_{i_1=1}^{3}\sum_{i_2=1}^{3} z_\alpha^{(i_1+i_2-1)} t\left\{\mu_{A_\alpha^{i_1}}(\lambda_k), \mu_{B_\alpha^{i_2}}(\Delta\lambda_k)\right\}}{\sum_{i_1=1}^{3}\sum_{i_2=1}^{3} t\left\{\mu_{A_\alpha^{i_1}}(\lambda_k), \mu_{B_\alpha^{i_2}}(\Delta\lambda_k)\right\}} \tag{5}$$

where t represents intersection operator and is chosen here as algebraic product.

3.2. Computation of Textural Weights

Texture is useful for discriminating between the contents of a complex scene and its important characteristics. Beside other approaches used for discriminating between the contents of a complex scene, Gray Level

Co-occurrence Matrix (GLCM) is most useful [25, 26]. The GLCM is based on the conjecture that the texture information is contained in an overall or average spatial relationship between the gray tones (in an image) [25, 26].

GLCM contains the conditional joint probabilities of intensity levels (p, q) of two pixels located at some distance and orientation. Here we choose unit distance and zero orientation (i.e., adjacent horizontal pixel) to generate co-occurrence matrix Θ_k of kth eigen image, i.e.,

$$\Theta_k(p,q) = \sum_{k_1=1}^{K-1} \sum_{l_1=1}^{L} \begin{cases} 1 & \text{for } G_k(k_1,l_1)=p \text{ and } G_k(k_1+1,l_1)=q \\ 0 & \text{otherwise} \end{cases} \tag{6}$$

To compute texture features from Θ_k statistical methods are used [25]. Although there are 14 textural features proposed by Haralick et al. in [26], but some of these features provide redundant information [26]. Here we use three Haralick features (correlation, energy and homogeneity). These three features provide distinct values for target and noise eigen images.

The correlation R_k of kth eigen image is,

$$R_k = \frac{\sum_p \sum_q \Theta_k(p,q) - a_1 a_2}{b_1 b_2} \tag{7}$$

where a_1, b_1 are row vectors containing means and variances of each row of kth eigen image. a_2, b_2 are column vectors containing means and variances of each column of kth eigen image. Since noise is uncorrelated so the eigen images containing noise have low correlation value.

The energy E_k of kth eigen image is,

$$E_k = \sum_p \sum_q \left(\Theta_k(p,q)\right)^2 \tag{8}$$

Noise subspaces have low energy as compared to target subspaces so for noise only subspaces value of E_k is low.

The homogeneity H_k of kth eigen image is,

$$H_k = \sum_p \sum_q \frac{\Theta_k(p,q)}{1+|p-q|} \tag{9}$$

Homogeneity provides the roughness in the image and noise eigen images have more roughness compared to target eigen images.

TS fuzzy system is used to compute weight β_k from above discussed (R_k, E_k and H_k) features for kth eigen image.

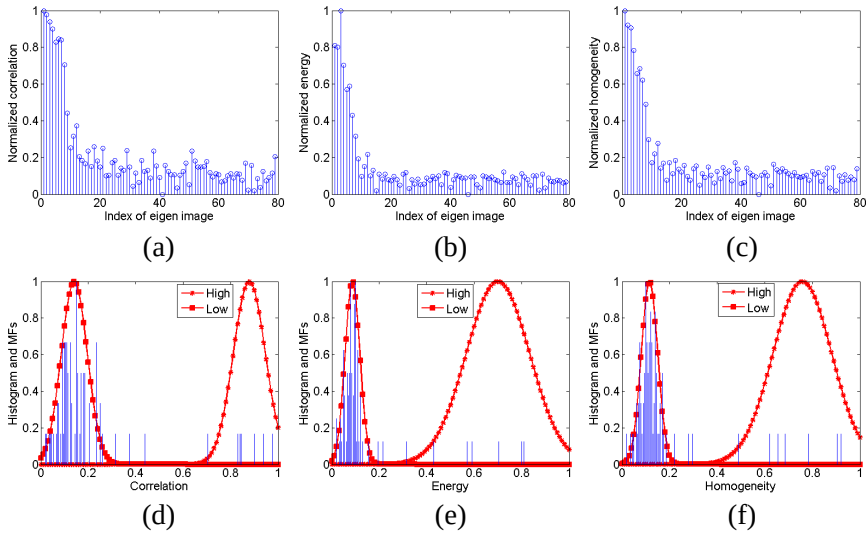

Figure 4. (a) Normalized correlation of eigen images. (b) Normalized energy of eigen images. (c) Normalized homogeneity of eigen images. (d) Histogram and MFs of correlation. (e) Histogram and MFs of energy. (d) Histogram and MFs of homogeneity.

Let, A_β^1 and A_β^2 represent "High" and "Low" respectively for R_k. The Gaussian MFs are $\mu_{A_\beta^1}(y_1) = \exp(-(\frac{y_1-\bar{y}_1^{(1)}}{\varrho_1^{(1)}})^2)$ and $\mu_{A_\beta^2}(y_1) = \exp(-(\frac{y_1-\bar{y}_1^{(2)}}{\varrho_1^{(2)}})^2)$. Let, B_β^1 and B_β^2 represent "High" and "Low" respectively for E_k. The Gaussian MFs are $\mu_{B_\beta^1}(y_2) = \exp(-(\frac{y_2-\bar{y}_2^{(1)}}{\varrho_2^{(1)}})^2)$ and $\mu_{B_\beta^2}(y_2) = \exp(-(\frac{y_2-\bar{y}_2^{(2)}}{\varrho_2^{(2)}})^2)$. Similarly, let C_β^1 and C_β^2 represent "High" and "Low" respectively for H_k. The Gaussian MFs are $\mu_{C_\beta^1}(y_3) = \exp(-(\frac{y_3-\bar{y}_3^{(1)}}{\varrho_3^{(1)}})^2)$ and $\mu_{C_\beta^2}(y_3) = \exp(-(\frac{y_3-\bar{y}_3^{(2)}}{\varrho_3^{(2)}})^2)$, where $\{y_1, y_2, y_3\} \in [0, 1]$. The means $\bar{y}_1^{(j_1)}$, $\bar{y}_2^{(j_2)}$, $\bar{y}_3^{(j_3)}$ and variances $\varrho_1^{(j_1)}$, $\varrho_2^{(j_2)}$, $\varrho_2^{(j_3)}$ for $\{j_1, j_2, j_3\} \in \{1, 2\}$ of fuzzy sets are determined using K-means algorithm as shown in Figure 4. The TS rule base for computing

textural weights is,

$$\text{IF } R_k \text{ is } A_\beta^{(j_1)} \text{ AND } E_k \text{ is } B_\beta^{(j_2)} \text{ AND } H_k \text{ is } C_\beta^{(j_3)}$$
$$\text{THEN } z_\beta^{(j_1+j_2+j_3-2)} = \left(\frac{1}{1+e^{-\varsigma_1 R_k}+e^{-\varsigma_2 E_k}+e^{-\varsigma_3 H_k}}\right)^{j_1+j_2-2} \quad (10)$$

where, ς_1, ς_2 and ς_3 are constants used to control the contribution of R_k, E_k and H_k respectively. Note that large $j_1 + j_2 + j_3$ reduces the output of rule base (textural weights) which is desirable.

The aggregated textural weight w_k^β is,

$$\beta_k = \frac{\sum_{j_1=1}^{2}\sum_{j_2=1}^{2}\sum_{j_3=1}^{2} y^{(i_1+i_2-1)} t\left\{\mu_{A_\beta^{j_1}}(R_k), \mu_{B_\beta^{j_2}}(E_k), \mu_{C_\beta^{j_3}}(H_k)\right\}}{\sum_{j_1=1}^{2}\sum_{j_2=1}^{2}\sum_{j_3=1}^{2} t\left\{\mu_{A_\beta^{j_1}}(R_k), \mu_{B_\beta^{j_2}}(E_k), \mu_{C_\beta^{j_3}}(H_k)\right\}} \quad (11)$$

4. SIMULATION RESULTS

Experimental setup for TWI consists of Agilents's Vector Network Analyzer (VNA) that generate stepped frequency waveforms 2 GHz–3 GHz (1 GHz Band Width (BW)) with step size $\Delta f = 5$ MHz and $N_f = 201$. Maximum scan range is,

$$R_{\max} = \frac{c(N_f - 1)}{2BW} = 30\,\text{m} \quad (12)$$

and the range resolution is,

$$\Delta R = \frac{c}{2N_f \Delta f} = 0.15\,\text{m} \quad (13)$$

Broadband horn antenna with directional beam and 12 dB gain is used in mono-static mode. For scanning along cross range and height, antenna is mounted on scanning frame (dimensions width 2.4 m and height 3 m) which can slide along cross range and height. Pyramidal radar absorbers are used to cover rear and side walls. Scanning steps are controlled by micro-controller and at each step scattering parameters are recorded by VNA and are transferred to computer for further processing. The antenna is kept 0.03 m away from the wall. Inverse Fourier transform is used to convert received frequency domain data to time domain. For image reconstruction, weights and propagation time delays are fed into beamforming algorithm.

The proposed and existing schemes are compared on the basis of Mean Square Error (MSE) [14], Peak Signal to Noise Ratio

(PSNR) [14], Improvement Factor (IF), Miss Detection (MD) and False Detection (FD). MD is defined as "target was present in the original image, but was not detected in enhanced image". FD is defined as "target was not present in the original image, but was detected in enhanced image".

IF is defined as,

$$\mathrm{IF} = 10 \log_{10} \left[\frac{P_{G_{tar},t} - P_{G,c}}{P_{G,t} - P_{G_{tar},c}} \right] \tag{14}$$

where $G_{tar} \in \{G_{tar_1}, G_{tar_2}, G_{tar_3}\}$. $P_{G_{tar},t}$ and $P_{G_{tar},c}$ are average pixel values of target and clutter in enhanced image respectively. $P_{G,t}$ and $P_{G,c}$ are average pixel values of target and clutter in original image, respectively.

Several experiments were conducted. One example is explained in

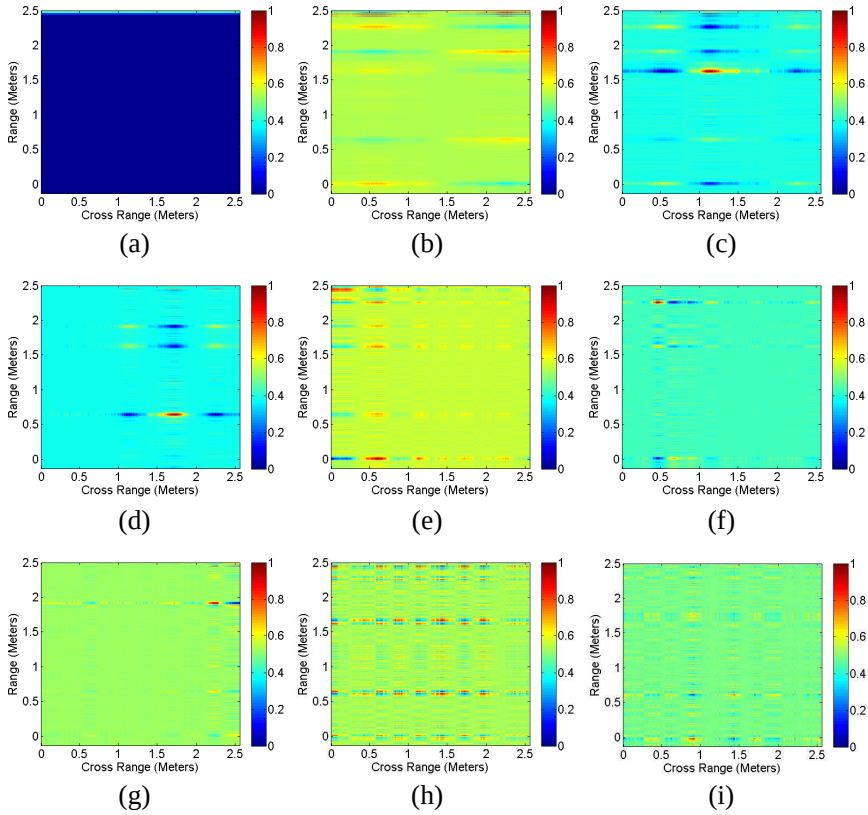

Figure 5. First nine eigen components of image containing five targets.

detail. Moreover, summary results for four examples having multiple rectangular shape targets (of size 0.15 m × 0.27 m at different locations) and two examples with single circular shape target (metallic and teflon having approximate diameters of 0.183 m and 0.122 m respectively) are given.

Figure 5 shows first nine eigen components of B-scan image containing five targets in it. Clearly first image (Figure 5(a)) contains wall clutter. Remaining eigen images contain target and noise information (Figures 5(b)–(i)). Note that eigen images also contain target information which motivate us to extract features (from eigen images) for calculating textural weights. In contrast to eigen values (that are placed in descending order), textural features computed using eigen images may not necessarily follow the same order. Therefore the

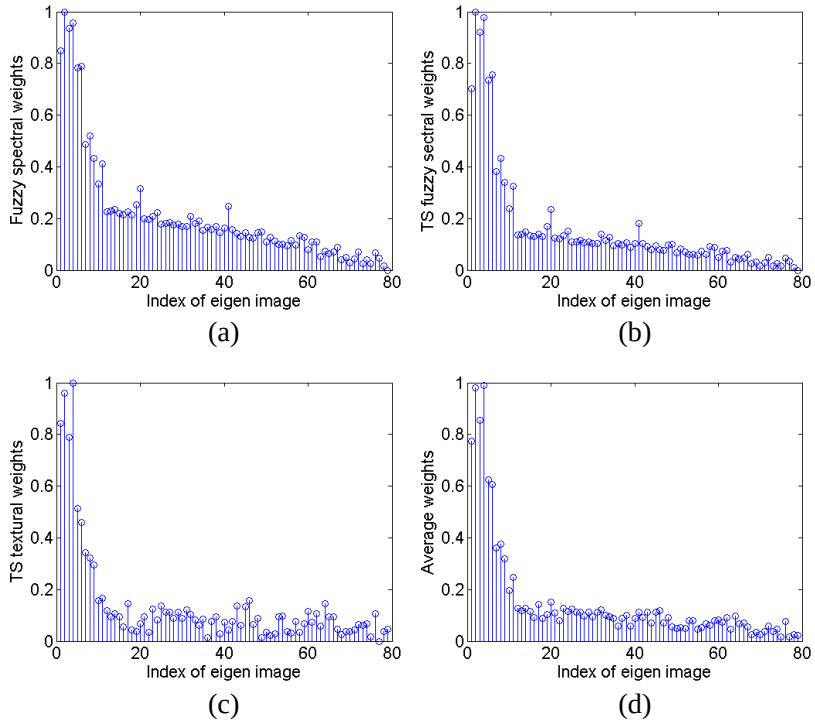

Figure 6. (a) Spectral weights obtained using FPCA [14]. (b) Spectral weights obtained using proposed scheme. (c) Textural weights obtained using proposed scheme. (d) Average of spectral and textural weights using proposed scheme.

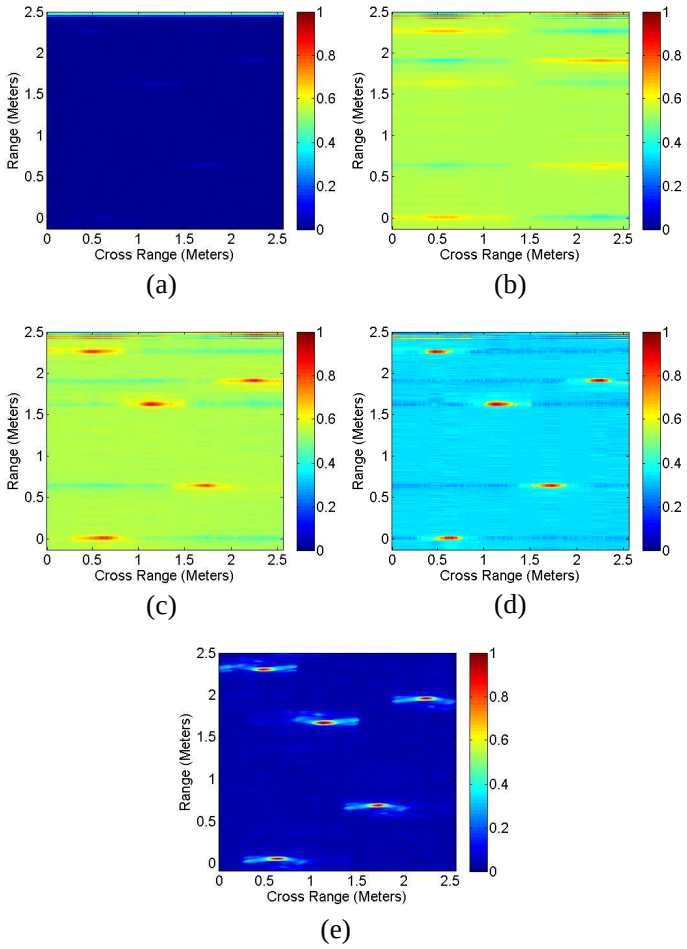

Figure 7. Images containing five targets. (a) Original *B*-scan image (b) Enhanced image using PCA [15]. (c) Enhanced image using FPCA [14]. (d) Enhanced image using proposed scheme. (e) Background subtracted image.

use of multiple features along with eigen values help in accurate weight assignment.

Figure 6(a) shows the weights computed using existing Fuzzy PCA (FPCA) scheme [14]. Figures 6(b)–(d) show the weights computed using spectral, textural and their combination respectively using proposed scheme. The effects of these weights on the results can be seen in Figure 7.

Figure 7(a) and Figure 7(e) show correspondingly the B-scan and background subtracted image containing five targets. Background subtracted image (calculated using difference of two images i.e., image with and without target) is used as reference image for calculating MSE and PSNR values [8]. Figures 7(b)–(d) correspondingly show the enhanced images using PCA [15], FPCA [14] and proposed TSPCA schemes. Note that PCA [15] scheme detects three targets only. Although other schemes have detected all targets successfully, however

Table 1. MSE, PSNR, IF, MD and FD for multiple targets using PCA [15], FPCA [14] and proposed TSPCA.

Number of Targets	Techniques	Measures				
		MSE	PSNR	IF	MD	FD
Two	PCA [15]	0.1532	8.1474	10.2574	0	1
	FPCA [14]	0.1410	8.5078	12.1163	0	0
	TSPCA	0.1018	9.9225	17.6769	0	0
Three	PCA [15]	0.1778	7.5007	10.1401	1	2
	FPCA [14]	0.1502	8.2333	12.0887	0	0
	TSPCA	0.1154	9.3779	17.5523	0	0
Four	PCA [15]	0.1961	7.0752	9.8541	2	2
	FPCA [14]	0.1631	7.8755	11.6711	0	0
	TSPCA	0.1231	9.0974	17.3104	0	0
Five	PCA [15]	0.2301	6.3808	9.6470	2	2
	FPCA [14]	0.1776	7.5056	11.1992	0	0
	TSPCA	0.1297	8.8706	17.1287	0	0

Table 2. MSE, PSNR and IF for single target using PCA [15], FPCA [14] and proposed TSPCA.

Types	Techniques	Measures		
		MSE	PSNR	IF
Metallic	PCA [15]	0.2569	5.9024	8.1129
	FPCA [14]	0.1987	7.0180	11.3233
	TSPCA	0.1368	8.6391	15.7956
Teflon	PCA [15]	0.3672	4.3510	5.2108
	FPCA [14]	0.2180	6.6154	7.3997
	TSPCA	0.1519	8.1844	11.2156

it is easy to note that the target to background ratio of image obtained using proposed TSPCA scheme is closer to background subtracted image.

Table 1 compares summary of MSE, PSNR, IF, MD and FD for multiple targets using PCA [15], FPCA [14] and proposed scheme. Clearly, MSE, PSNR, IF, MD and FD are much improved using proposed scheme.

Table 2 compares summary of MSE, PSNR and IF for single circular shape (metal and teflon) target using PCA [15], FPCA [14] and proposed scheme. Clearly, proposed TSPCA scheme produces improved results.

5. CONCLUSION

A TWI image enhancement scheme involving TS fuzzy system and PCA is proposed. Spectral properties of image and textural properties of eigen images are used for assigning weights to different components. The scheme overcomes the empirical setting of inference engine and output MFs. Effectiveness of proposed scheme in terms of accuracy is demonstrated via simulation results.

REFERENCES

1. Amin, M. G., *Through the Wall Radar Imaging,* CRC press, USA, 2011.
2. Jia, Y., L. Kong, and X. Yang, "A novel approach to target localization through unknown walls for through-the-wall radar imaging," *Progress In Electromagnetics Research*, Vol. 119, 107–132, 2011.
3. Zhang, W., A. Hoorfar, and L. Li, "Through-the-wall target localization with time reversal music method," *Progress In Electromagnetics Research*, Vol. 106, 75–89, 2010.
4. Zheng, W., Z. Zhao, and Z. P. Nie, "Application of TRM in the UWB through wall radar," *Progress In Electromagnetics Research*, Vol. 87, 279–296, 2008.
5. Zhu, F., S. C. Gao, A. T. S. Ho, T. W. C. Brown, J. Li, and J. D. Xu, "Low-profile directional ultra-wideband antenna for see-through-wall imaging applications," *Progress In Electromagnetics Research*, Vol. 121, 121–139, 2011.
6. Yang, Y., Y. Wang, and A. E. Fathy, "Design of compact Vivaldi antenna arrays for UWB see through wall applications," *Progress In Electromagnetics Research*, Vol. 82, 401–418, 2008.

7. Zheng, W., Z. Zhao, Z. P. Nie, and Q. H. Liu, "Evaluation of TRM in the complex through wall environment," *Progress In Electromagnetics Research*, Vol. 90, 235–254, 2009.
8. Moulton, J., S. A. Kassam, F. Ahmad, M. G. Amin, and K. Yemelyanov, "Target and change detection in synthetic aperture radar sensing of urban structures," *Proceedings IEEE Radar Conference*, 1–6, May 26–30, 2008.
9. Yoon, Y. S. and M. G. Amin, "Spatial filtering for wall clutter mitigation in through-the-wall radar imaging," *IEEE Transactions on Geoscience and Remote Sensing*, Vol. 47, 3192–3208, 2009.
10. Dehmollaian, M. and K. Sarabandi, "Refocusing through building walls using synthetic aperture radar," *IEEE Transactions on Geoscience and Remote Sensing*, Vol. 46, 1589–1599, 2008.
11. Smith, G., and B. G. Mobasseri, "Robust through-the-wall radar image classification using a target-model alignment procedure," *IEEE Transactions on Image Processing*, Vol. 21, No. 2, 754–767, 2012.
12. Ram, S. S., C. Christianson, K. Youngwook, and L. Hao, "Simulation and analysis of human micro-dopplers in through-wall environments," *IEEE Transactions on Geosciences and Remote Sensing*, Vol. 48, 2015–2023, 2010.
13. Debes, C., "Advances in detection and classification for through the wall radar imaging," Ph.D. Dissertation, Technische University Darmstadt, 2010.
14. Riaz, M. M. and A. Ghafoor, "Principle component analysis and fuzzy logic based through wall image enhancement," *Progress In Electromagnetics Research*, Vol. 127, 461–478, 2012.
15. Verma, P. K., A. N. Gaikwad, D. Singh, and M. J. Nigam, "Analysis of clutter reduction techniques for through wall imaging in UWB range," *Progress In Electromagnetics Research B*, Vol. 17, 29–48, 2009.
16. Riaz, M. M. and A. Ghafoor, "Through wall image enhancement based on singular value decomposition," *International Journal of Antenna and Propagation*, 1–18, 2012.
17. Tivive, F. H. C., A. Bouzerdoum, and M. G. Amin, "An SVD-based approach for mitigating wall reflections in through-the-wall radar imaging," *IEEE Radar Conference (RADAR)*, 519–524, Kansas City, MO, USA, 2011.
18. Riaz, M. M. and A. Ghafoor, "Wavelet transform and principal component analysis based clutter reduction for through

wall imaging", *38th IEEE International Industrial Electronics Conference*, 1597–1602, Montreal, Canada, Oct. 25–28, 2012.

19. Tivive, F. H., M. G. Amin, and A. Bouzerdoum, "Wall clutter mitigation based on eigen analysis in through the wall radar imaging," *Digital Signal Processing*, 1–8, Corfu, Greece, 2011.
20. Riaz, M. M. and A. Ghafoor, "Fuzzy singular value decomposition based clutter reduction for through wall imaging," *IEEE International Conference on Ultra-Wideband (ICUWB)*, 106–110, Bologna, Italy, 2011.
21. Riaz, M. M. and A. Ghafoor, "Fuzzy logic and singular value decomposition based through wall image enhancement," *Radioengineering*, Vol. 22, No. 1, 580–589, 2012.
22. Wang, L. X., *A Course in Fuzzy Systems and Control*, Prentice Hall PTR, USA, 1997.
23. Kanungo, T., D. M. Mount, N. S. Netanyahu, C. D. Piatko, R. Silverman, and A. Y. Wu, "An efficient K-means clustering algorithm: Analysis and implementation," *IEEE Transactions Pattern Analysis and Machine Intelligence*, Vol. 24, 881–892, 2002.
24. Takagi, T. and M. Sugeno, "Fuzzy identification of systems and its applications to modeling and control," *IEEE Transactions on Systems, Man and Cybernetics*, Vol. 15, 116–132, 1985.
25. Haralick, R. M., K. Shanmugam, and I. H. Dinstein, "Textural features for image classification," *IEEE Transactions on Systems, Man and Cybernetics*, Vol. 6, 610–621, 1973.
26. Shanmugan, K. S., V. Narayanan, V. S. Frost, J. A. Stiles, and J. C. Holtzman, "Textural features for radar image analysis," *IEEE Transactions on Geoscience and Remote Sensing*, Vol. 3, 153–156, 1981.